Magnetohydrodynamics at Heavy Ion Collisions

Eric Marcus*

Supervisors: dr. Umut Gürsoy[1] & prof. dr. Raimond Snellings[2]
[1] *Institute for Theoretical Physics, Utrecht University*
[2] *Institute for Subatomic Physics, Utrecht University*

ABSTRACT
Quantum Chromo Dynamics predicts a phase transition from hadronic matter to a system with new degrees of freedom at temperatures accessible in laboratory. This state of matter, called the Quark Gluon Plasma (QGP), is created at Heavy Ion Collisions. In these collisions there should be large electromagnetic fields present that affect the evolution of the QGP. After obtaining the electromagnetic fields we study the effects of the fields on the QGP. The influence is studied using relativistic viscous hydrodynamics. We show the influence on the anisotropic flow of the QGP, in particular the directed flow, elliptic flow and triangular flow.

Keywords
Electromagnetic fields, Quark-Gluon plasma, Hydrodynamics, Anisotropic flow, Heavy Ion Collisions

INTRODUCTION
In this section we will explain what Heavy Ion Collisions are, why we are interested in them and how the electromagnetic fields arise. Apart from these subjects we will also give a short introduction to anisotropic flow. The QGP consists, as its name suggests, of quarks and gluons. These are fundamental building blocks of the world we know. It is hypothesized that this QGP existed for several microseconds after the big bang. It is also possible that the QGP might be present in the cores of neutron stars [1]. There are thus enough reasons to thoroughly study this phase of matter. The laboratory where this is best studied is the ALICE experiment at CERN Switzerland, where heavy ions are collided. An example of a heavy ion collision is given in Figure 1. An important tool used in these collisions is the centrality, which states how peripheral the collision was.
Now that we know what these collisions look like, we can investigate the origin of induced currents in the QGP. First there is an electromagnetic field due to the moving spectators. This can be seen from the fact that moving charges (here: spectators) generate (besides their usual electric field) a magnetic field. When the spectators move away from the QGP their electromagnetic field drops, and thus changes in time. From classical electrodynamics we know that a changing magnetic field will result in an electric field, the induced Faraday current. Second there is the Hall effect that is induced due to the Lorentz force $\vec{F} = q\vec{E} + q\vec{v}\times\vec{B}$. This force is thus perpendicular to the longitudinal speed and the B-field. The Hall effect occurs because charged particles of different sign are directed to opposite sides, which in turn generates another electric field.

*Contact: ericj.marcus@gmail.com

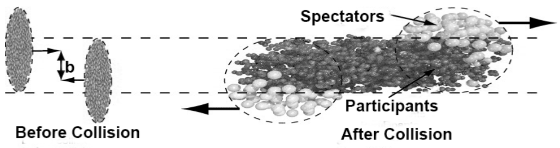

Figure 1: The left side shows the Lorentz-contracted blobs of protons before the collision, where b defines the impact parameter. On the right hand side, the situation after the collision is shown. The participants are the particles that participate in the collision and the spectators are the particles that fly by the collision. Figure from Ref. [1].

Our eventual goal will be to find out what the influence of these electromagnetic fields is on the evolution of the QGP. This evolution of the QGP can be constrained by determining the so-called anisotropic flow. Anisotropic flow has different forms which provide information on the bulk properties of the matter and the initial geometry of the collision. The most prominent anisotropic flows we look at are the directed, elliptic and triangular flow, noted by v_1, v_2 and v_3 respectively. These flow components originate from a Fourier expansion of the particle spectrum, shown in Equation 1. We note that for later purposes, we are only interested in the small contribution to the anisotropies caused by the electromagnetic fields. This charge-dependent contribution is smaller than the total flow caused by the hydrodynamical response to the initial asymmetries.

$$E\,\frac{d^3N}{dp^3} = \frac{1}{2\pi}\,\frac{d^2N}{dp_T\,dY}\left(1 + 2\sum_{n=1}^{\infty} v_n\,\cos[n(\phi - \psi_{RP})]\right) \quad (1)$$

Where E is the energy, p the momentum, p_T the transverse momentum and Y the rapidity. ψ_{RP} is the angle with the Reaction Plane (which we pick zero for our theoretical model) and, most importantly, v_n are the flow harmonics. From this expansion we can derive the properties of the different flows. The directed flow is the flow directed along transverse axes with respect to the beam axis. The elliptic flow is the elliptic expansion of the plasma in the transverse plane, as shown in Figure 2, so proportional to $cos(2\,\phi)$. The triangular flow then shows us characteristics with respect to $cos(3\,\phi)$ (resulting in a triangle shape, hence it's name).

So in summary, Equation 1 shows us that we can figure out the details of the expansion of the QGP in terms of our anisotropic flow harmonics.

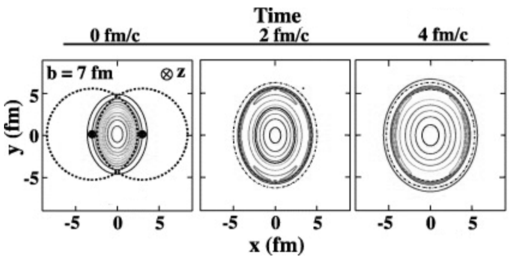

Figure 2: Shown here is the elliptic flow and its time dependence. One can see the characteristic elliptic shape of the expansion which defines elliptic flow. Note that the z-direction is the beam direction.

METHODS

Electromagnetic fields

We obtain expressions for the EM fields by using the Maxwell equations and including a constant conductivity by Ohm's law $\vec{J} = \sigma \vec{E}$, picked as $\sigma = 0.023$ fm^{-1} [2]. These equations yield a differential equation as shown below.

$$\vec{\nabla}^2 \vec{B} - \frac{\partial^2 \vec{B}}{\partial t^2} - \sigma \frac{\partial \vec{B}}{\partial t} = -e\, v\, \vec{\nabla} \times (\hat{z} \delta(z - vt) \delta(\vec{x}_\perp - \vec{x}'_\perp))$$

The coordinate with the apostrophe denotes the location of the particle that creates the field. As it turns out, solving this equation is not trivial. We solved it using Green's functions, complex analysis and integral definitions. The result obtained for the magnetic field (in $\hat{y}$ direction) is shown in Equation 2.

$$e\vec{B}_y^+(\tau, \eta, x_\perp, \phi) = \alpha_{em}\, \hat{y}\, \sinh(Y)\, (x_\perp \cos(\phi) - x'_\perp \cos(\phi')) \times \frac{\left(\frac{\sigma\, |\sinh(Y)|}{2} \sqrt{\Delta} + 1\right)}{\Delta^{\frac{3}{2}}}\, e^A \qquad (2)$$

The + represents the fact that it is a positively moving ($+\hat{z}$) particle and Y denotes the rapidity. Note that we work in Bjorken coordinates, so η is pseudorapidity and $x_\perp$ is the equivalent of $\sqrt{x^2 + y^2}$ in Cartesian coordinates. We have defined A and Δ as follows:

$$A = \frac{\sigma}{2} (\sinh(Y)\, \sinh(Y - \eta) - |\sinh(Y)|\, \sqrt{\Delta})$$
$$\Delta = \tau^2\, \sinh^2(Y - \eta) + (x_\perp)^2 + (x'_\perp)^2 - 2\, x_\perp\, x'_\perp\, \cos(\phi - \phi')$$

The same solving procedure can be used to solve the for the electric field, which yields the result:

$$eE_x = e\, B_y\, \coth(Y - \eta) \qquad (3)$$

The other components of the electromagnetic field are irrelevant since $B_z = 0$. To obtain now the total contribution of all particles we need to integrate over the coordinates indicated with an apostrophe in Equation 2 with some distribution function. For the participants we also need to include the loss of rapidity in the collision. In both cases we assumed that the particles were evenly distributed over a sphere with radius $R = 7$ fm. We then assumed that our impact parameter (distance between centers) was $b = 7$ fm, or in other words we use 20-30% centrality. Using the distribution the limits of the $x'_\perp$ integrals can be found. For the participants we integrate over the part that will overlap, for spectators we integrate over the non-overlapping area.

Hydrodynamics

Before we can make use of the derived electromagnetic fields we first need to simulate the 'normal' expansion of the QGP. Where 'normal' means thus the expansion without any of the effects of the EM fields. To do this we used a model created by Gubser in 2010 [3]. In practice this model gives us the local fluid temperature and the four velocity u^μ which describes the fluid velocity of our QGP, Equation 4. Note that Gubser's model is azimuthally symmetric and boost invariant and therefore does not have u^ϕ and u^η.

$$u^\tau = \frac{1 + q^2 \tau^2 + q^2 x_\perp^2}{2\, q\, \tau \sqrt{1 + g^2}} \quad ; \quad u^\perp = \frac{q\, x_\perp}{\sqrt{1 + g^2}} \qquad (4)$$

Here, q is a parameter (that we have to pick) proportional to the inverse length and the variable g is given in Equation 5.

$$g = \frac{1 + q^2\, x_\perp^2 - q^2\, \tau^2}{2\, q\, \tau} \qquad (5)$$

The next thing to introduce is the freezeout of the QGP. The local fluid temperature allows us to find isothermal curves in the model parameterized as $\tau(x_\perp)$ (τ is proper time). One important curve will be at the freezeout temperature. We choose to pick $T_f = 130$ MeV. The hydrodynamics that are developed deal with quantities like energy density and fluid velocity. The experiment, however, deals with measured quantities like the momentum spectra of protons and pions. The link between the hydrodynamic variables and the desired spectra (Equation 1) is then given by the Cooper-Frye freezout procedure [4]. In summary we can write it as Equation 6, where we assumed that we have a Boltzmann distribution function.

$$S_i = \left(p^0 \frac{d^3\, N_i}{d^3\, p} \right) = -\frac{d_i}{(2\pi)^3} \int d\Sigma_\mu\, p^\mu e^{\frac{p^\mu\, u_\mu}{T_f}} \qquad (6)$$

Note that d_i is the degeneracy of the particle, $d\Sigma_\mu$ is an area element of the freezeout surface, T_f the freezeout temperature and p^μ is the four momentum. We expect the freezeout to happen when the temperature becomes so low that the interactions can no longer hold thermal equilibrium. For our QGP, this happens as it cools and the viscosity becomes stronger, until the viscous corrections cause the hydrodynamic description to be no longer viable, see also [5]. For our used hydrodynamic model we know, however, that it is azimuthally symmetric. When we then look at Equation 1 we see that the only non-zero flow harmonic will be v_0. This v_0 essentially describes our expansion without any of the electromagnetic effects. By fixing the parameters in the model we tried to obtain a spectrum as close to the experimental spectrum of ALICE [6] as possible.

Obtaining the anisotropic flow

In order to obtain the flow harmonics, we need the fluid velocity V^μ, which contains both the expansion due to Gubser's model and the contribution of the electromagnetic field. We do this by doing a Lorentz boost to the local fluid restframe in which applies $u'^\mu = 0$. At this point we shall solve the equation of motion given in Equation 7, to get the velocity due to the electromagnetic fields $\vec{v}'$.

$$m \frac{d\vec{v}'}{dt} = q\vec{E}' + q\vec{v}' \times \vec{B}' - \mu\, m\, \vec{v}' = 0 \qquad (7)$$

The first term indicates the Lorentz force and the second term the drag force. The drag coefficient μm we choose to obtain from $N = 4$ supersymmetric Yang-Mills (SYM) theory. We do this to keep an analytic solution. The drag force coefficient is currently only known precisely for heavy quarks in the $N = 4$ SYM theory [7].

$$\mu m = \frac{1}{2}\,\pi\,\sqrt{\lambda}\,T^2 \tag{8}$$

Where $\lambda = g^2\,N_c$, called the t' Hooft coupling. Here g is the gauge coupling and N_c the number of colors. We shall pick just as in [2], $\lambda = 6\pi$ and $T = \frac{3}{2}\,T_c$, where T_c is the crossover temperature to hadrons.

We now solve Equation 7 for up quarks ($q = \frac{2}{3}e$) and anti down quarks ($q = \frac{1}{3}e$), which will be combined to get results for positively charged particles. We simply add the two found velocities together and divide by two to get our final velocity. For negatively charged particles we use the down and anti up quarks. Note that we assume that there are equal distributions of up and down quarks and thus ignore any chemical potential induced by the differences. The negative particles will just be characterized by $-\vec{v}'$. When we have solved this equation we can boost back to the original frame, again including the u^μ and obtaining our final four velocity V^μ. We now rewrite Equation 1 with the assumption $\psi_{RP} = 0$ to obtain a general expression for v_n, with $n \geq 1$.

$$v_n(p_T, Y) = \frac{\int_{-\pi}^{\pi} d\phi_p \cos(n\phi_p) S_i(p_T, Y, \phi_p)}{2\pi v_0} \tag{9}$$

We can take the v_0 (in the numerator) to be only due to the hydrodynamic model since we will find that the electromagnetic contribution to this is minimal. So all we need now is an expression for S_i and we are capable to compute our flow harmonics. The procedure to obtain this is already outlined in Equation 6, but instead of u^μ we use now V^μ. The results of these calculations are shown in Equation 10.

$$\begin{aligned}
&\int_{-\pi}^{\pi} d\phi_p \cos(n\phi_p)\, S_i(p_T, Y, \phi_p) = \frac{d_i}{(2\pi)^3} \int d\eta dx_\perp d\phi \\
&\times x_\perp \tau_f(x_\perp) \left[e^{-\frac{m_T}{T_f}(V^\tau \cosh(Y-\eta) - V^\eta \tau_f \sinh(Y-\eta))} \right. \\
&\left. \times \left(m_T \cosh(Y-\eta) M_n + R_f\, p_T N_n \right) \right]
\end{aligned} \tag{10}$$

Where $\tau_f(x_\perp)$ is the freezeout proper time, R_f is given by the ratio $R_f = -\partial\tau_f(x_\perp)/\partial x_\perp$ and $m_T = \sqrt{m^2 + p_T^2}$. The p_T is the momentum in the transverse plane (so perpendicular to the beam axis). Furthermore, M_n and N_n read:

$$\begin{aligned}
M_n &= 2\pi \cos(n(\phi + \xi))\, I_n(\zeta) \\
N_n &= \pi \left(\cos[(n-1)\xi + n\phi]\, I_{n-1}(\zeta) \right. \\
&\quad \left. + \cos[(n+1)\xi + n\phi]\, I_{n+1}(\zeta)\right)
\end{aligned}$$

Here I denote Bessel functions. Furthermore, we have $\xi = \arctan\left(\frac{B}{A}\right)$ and $\zeta = \sqrt{A^2 + B^2}$ with:

$$A \equiv \frac{p_T\, V^\perp}{T_f}, \qquad B \equiv \frac{p_T\, V^\phi\, x_\perp}{T_f}$$

RESULTS

Flow harmonics

To obtain the final results for our flow harmonics we need to complete the integrals in Equation 10 and divide by $2\pi v_0$. As it turns out these remaining integrals will have to be solved numerically. As can be seen from these expressions the eventual flow harmonics will be dependent on the rapidity Y and the transverse momentum p_T. We used the described methods to obtain results for pions and protons. We show here the results for pions; directed flow in Figure 3, elliptic flow in Figure 4 and the triangular flow in Figure 5.

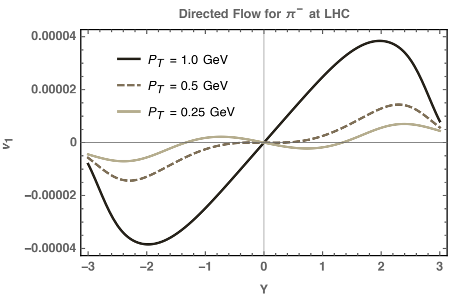

Figure 3: The directed flow at fixed transverse momentum for π^-. Results for π^+ have the same magnitude but opposite sign, showing the charge-dependency.

The directed and triangular flow are asymmetric in rapidity whilst the elliptic flow is not. This can also be related to the respective angle dependencies and we can in fact expect that all even harmonics will be symmetric in Y.

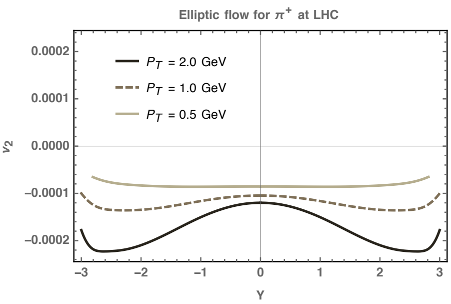

Figure 4: The elliptic flow at fixed transverse momentum for π^+. Note that this is no longer asymmetric in rapidity. Just as with v_1, the results for π^- are exactly opposite.

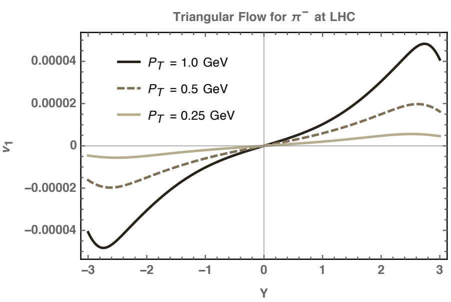

Figure 5: Here we show the triangular flow v_3 at fixed P_T for π^-. It has about equal order of magnitude as v_1.

One thing we notice is that the elliptic flow is about one order of magnitude larger than both the directed and triangular flow. Note again that these results for v_1, v_2 and v_3 are due to the electromagnetic effects only. In reality there will be a larger contribution due to initial asymmetries in the collision.
Apart from looking at fixed transverse momenta we have also obtained results for the flows integrated over certain p_T bins. We show an example in Figure 6 where we integrated from 0.5 GeV to 5.0 GeV. As can be seen the effect increases by around a factor of two.

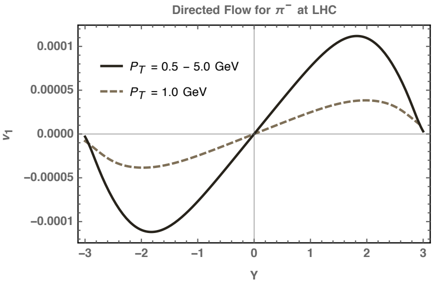

Figure 6: The directed flow integrated over the transverse momentum. We use this particular p_T range since it is often used in experiment.

We now look into the effect of some of our most important parameters in these calculations. The two most important parameters are the conductivity of the QGP and the drag force coefficient μm as seen in Equation 7. The results of conductivity are shown in Figure 7, the drag force coefficient in Figure 8. For the conductivites we used Ref. [8] to approximate that $\sigma_{min} \simeq 0.0052 fm^{-1}$ and $\sigma_{max} \simeq 0.092 fm^{-1}$.

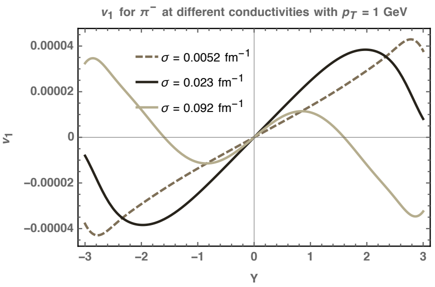

Figure 7: The directed flow for different conductivities of the QGP. The solid line ($0.023 fm^{-1}$) corresponds to earlier calculations. One sees that adjusting the σ results in moving the peak of v_1.

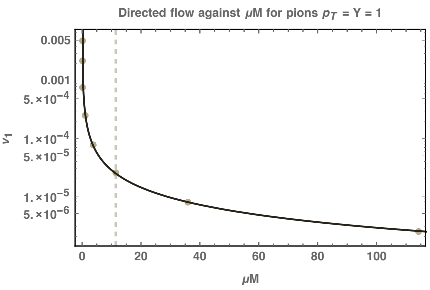

Figure 8: The directed flow v_1 plotted against the drag force coefficient. Note that $v_1 \propto \frac{1}{\mu m}$. The dashed curve indicates the value we used in previous calculations.

CONCLUSIONS

The results of our study show that the electromagnetic fields at HIC lead to a charge-dependent contribution to the expansion of the QGP. We can for v_1 conclude that the effect is rather small (around 0.0001). The triangular flow is of the same order of magnitude and both the v_1 and v_3 are asymmetric in rapidity. On the other hand, the elliptic flow is symmetric in rapidity and about one order of magnitude bigger than the other two found flow harmonics.

It can be seen that the drag force coefficient is by far the most influential parameter as $v_1 \propto \frac{1}{\mu m}$. So in the case of experimental differences in this effect close attention should be payed to the strong influence of this μm. The conductivity shows something similar to a general shift of the directed flow. Perhaps this effect can be used to constrain the actual conductivity of the QGP.

For further development in the project, we argue for the importance of a complete numerical hydrodynamic model. This numerical model would then include realistic background flow harmonics, which the analytic model by Gubser lacks. Another interesting addition could be the Chiral Magnetic Effect. This effect could result in a contribution to the magnetic fields and would add a necessary quantum approach to the currently completely classical computation.

Role of the student

Before the start of Eric's Honours-bachelor research U. Gürsoy, D. Kharzeev and K. Rajagopal had recently published a paper about the same topic, showing results for the directed flow. Supervised by R. Snellings and U. Gürsoy Eric continued on the research in the field. After redoing the calculations up to v_1 he corrected the expression for the general v_n. Eric then obtained the first results for v_2 and v_3. He also obtained the influences of several important parameters on the eventual results of the flow harmonics. During past year he regularly met with his supervisors to discuss and evaluate obtained results. The outcomes of the research were written up in a thesis, this paper is a short summary of that. Besides this also a paper co-written with the authors of the previous paper on this subject is in progress. The work on including the numerical background is also already in progress.

REFERENCES

[1] R. Snellings, "Elliptic flow: a brief review," New Journal of Physics, vol. 13, Article ID 055008, 2011.

[2] Umut Gürsoy et al., Magnetohydrodynamics, charged current and directed flow in heavy ion collisions. Phys. Rev. C 89, 054905 (2014)

[3] S. S. Gubser, Phys. Rev. D 82, 085027 (2010) [arXiv:1006.0006 [hep-th]].

[4] F. Cooper and G. Frye, Phys. Rev. D 10, 186 (1974).

[5] P. Romatschke "New developments in relativistic viscous hydrodynamics" Int.J.Mod.Phys.E19:1-53,2010 [arXiv:0902.3663 [hep-ph]]

[6] B. Abelev et al. [ALICE Collaboration], Phys. Rev. C 88, 044910 (2013) [arXiv:1303.0737 [hep-ex]].

[7] C. P. Herzog, A. Karch, P. Kovtun, C. Kozcaz and L. G. Yaffe, JHEP 0607, 013 (2006) [hep-th/0605158].

[8] A. Amato, G. Aarts, C. Allton, P. Giudice, S. Hands and J. -I. Skullerud, Phys. Rev. Lett. 111, 172001 (2013) [arXiv:1307.6763 [hep-lat]].